Entrainment Characteristics of Fine Particles in Cylindrical and Conical Inert-Medium Fluidized Beds

ARTICLE *in* INDUSTRIAL & ENGINEERING CHEMISTRY RESEARCH · FEBRUARY 2007

Impact Factor: 2.59 · DOI: 10.1021/ie061098e

7 AUTHORS, INCLUDING:

Dong Hyun Lee
Asan Medical Center
327 PUBLICATIONS **3,581** CITATIONS
SEE PROFILE

Sang Done Kim
Korea Advanced Institute of Science and Tec…
365 PUBLICATIONS **5,559** CITATIONS
SEE PROFILE

Entrainment Characteristics of Fine Particles in Cylindrical and Conical Inert-Medium Fluidized Beds

Moon Kwon Shin, Eun Mi Kim, Bon Seok Koo, Gui Young Han, Ki June Yoon, and Dong Hyun Lee*

Department of Chemical Engineering, Sungkyunkwan University, Suwon, 440-746 Korea

Sang Done Kim

Department of Chemical and Biomolecular Engineering and Energy and Environment Research Center, Korea Advanced Institute of Science and Technology, Daejeon, 305-701, Korea

The entrainment characteristics of fine powder from solid mixtures (Geldart groups A and C) in the gas−solid fluidized beds were determined in a conical fluidized bed (cone angle = 10°) and a cylindrical fluidized bed (inner diameter of 0.1 m) with or without a tube (outer diameter of 0.06 m). Alumina particles (group A) were used as the inert medium, and carbon black particles were used as the fine powder (group C). The entrainment rate of fine powders was determined by measuring the initial weight loss from the bed. The effects of gas velocity, the content of carbon black in mixed-bed materials, the type of reactor (conical and cylindrical), and the static bed height on the entrainment rate were determined. The entrainment rate increased as the gas velocity increased but decreased as the content of fine powders in the cylindrical fluidized beds increased. At a given gas flow rate, the entrainment rate constants from cylindrical fluidized beds were 5−12 times higher than those of conical fluidized beds.

1. Introduction

Direct decarbonization is currently being evaluated for hydrogen production in which pure hydrogen is produced without CO_2 formation. Moreover, this method produces pure carbon black that has various applications. For continuous hydrogen production processes, it is necessary to entrain carbon black continuously during the reaction, to prevent the accumulation of carbon black that is created inside the hydrogen production reactor.

It is well-known that the entrainment rate constant of Geldart group A particles is affected by the properties of entrained particles and by the operating parameters.[1,2] However, Li et al.[3] reported that the entrainment rate constant of Geldart group C powders is also affected by the weight fraction of the entrained powder in the bed (i.e., the mean diameter of the bed particles). The entrainment rate constant of Geldart group C powders was determined to decrease with increasing mean diameters of the bed particles at a given gas velocity,[4,5] and it has been observed to differ from those of Geldart group A or group B particles. However, previous studies have not provided information on the interaction of small particle size powders (Geldart group C) on the entrainment rates with Geldart group A or group B particles. Kato et al.[6] developed a powder-particle fluidized bed (PPFB) to treat group C powders by feeding the fine powders continuously into a fluidized bed of coarse particles (Geldart groups A and B). This technique has been utilized in various processes, such as the continuous drying of fine particle−water slurries,[7] the reduction of iron oxide fine particles from a converter,[8] the catalytic pyrolysis of coal and biomass,[9] and the simultaneous removal of SO_2 and NO using iron oxide dust as a sorbent.[10] Geldart and Wong[11] determined that the entrainment flux of alumina first increases and then decreases as the fines content increases, because cohesive powders have strong interparticle forces and also have a tendency to form larger powder sizes. Baron et al.[12] reported that the smallest particles are not the most easily entrained from a fluidized bed of mixed silica sand, FCC, and polyethylene particles, because of the agglomeration of fine powders.

In the present study, the entrainment characteristics of fine carbon black powders with solid mixtures were determined in conical and cylindrical fluidized beds with or without a tube.

2. Experimental Section

Experiments were conducted using a cylindrical fluidized bed composed of transparent acrylic (0.1 m inner diameter (ID) × 0.6 m height), as shown in Figure 1a. The cylindrical shape reactor can be transformed by replacing the lower portion of the reactor with a conical shape with a cone angle of 10° at its base, as shown in Figure 1b. All experiments were performed at room temperature and atmospheric pressure. Gas velocities were measured using an orifice-type flowmeter (FLT, Korea Flow Cell Co.) in the flow range of 0−0.065 m/s. The inlet air was dehumidified to 9.8% (relative humidity) by air dehumidified (JEMACO, model TX15K). The distributor used in the present study was a 1-mm perforated plate with an opening area ratio of 1.0%. In this case, a 400-mesh screen was used to cover the surface of a distributor, to prevent particle weeping from the bed to the plenum chamber. The solid particles used were carbon black (HI-900L, from Korea Carbon Black Co.), alumina (F-150, F-220), glass beads, and poly(vinyl chloride) (PVC) particles (see Table 1). Eleven pressure taps were mounted along the column axis to measure pressure in the conical and cylindrical fluidized beds (see Figure 1). As might be expected, fine carbon black powders (Geldart group C) cannot be easily fluidized by gas, because they are cohesive particles. Therefore, to improve fluidization quality, alumina (Geldart group A) particles were added into the bed of carbon black powders (HI-900L).

* To whom correspondence should be addressed. Tel: +82-31-290-7340. Fax: +82-31-299-4709. E-mail: dhlee@skku.edu.

10.1021/ie061098e CCC: $37.00
Published on Web 01/24/2007

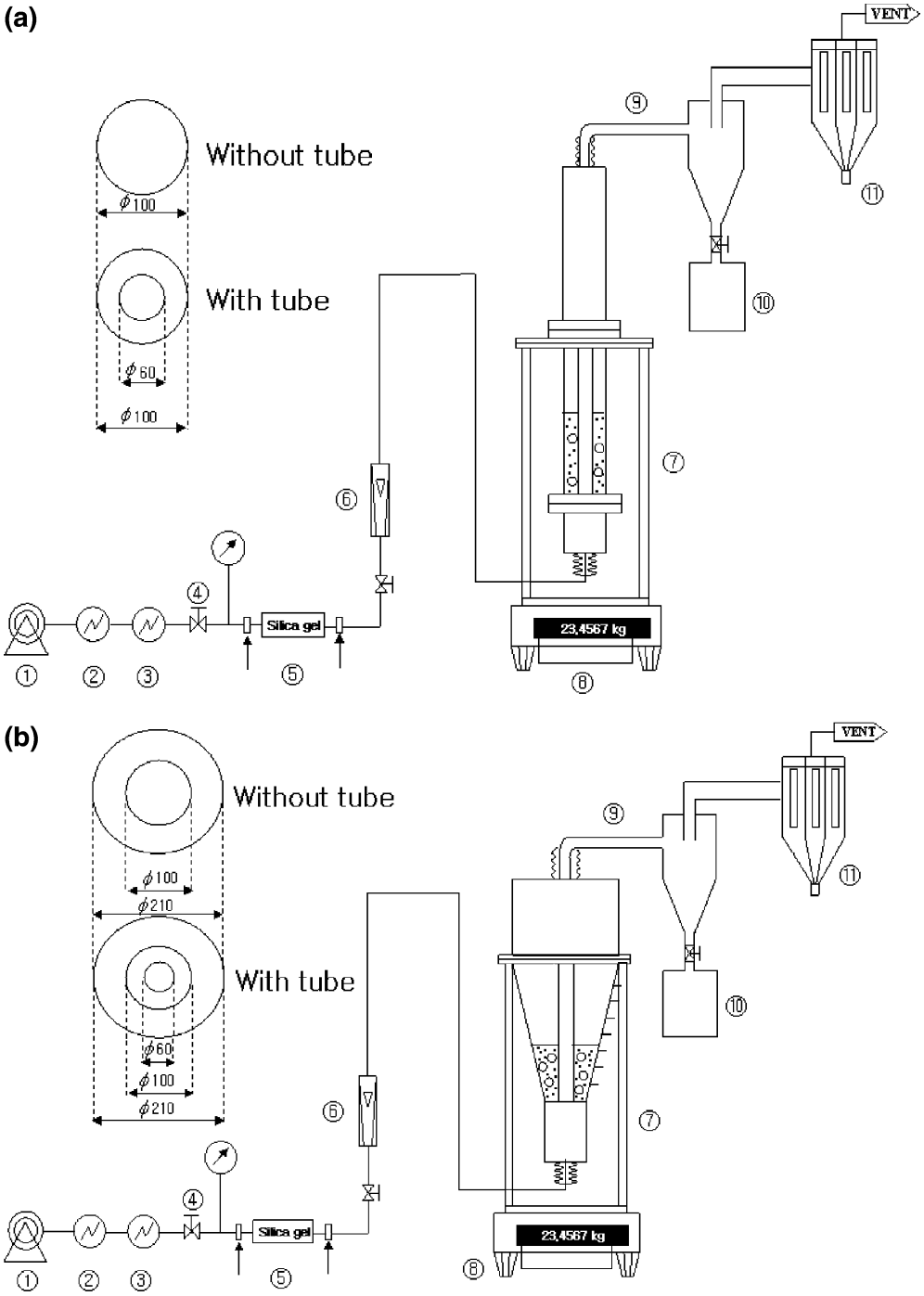

Figure 1. Schematic diagram of the experimental apparatus: (a) cylindrical fluidized-bed reactor and (b) conical fluidized-bed reactor. Legend: 1, compressor; 2, regulator; 3, mist separator; 4, pressure gauge; 5, dehumidifier; 6, flowmeter; 7, cylindrical column (in panel a) or conical column (in panel b); 8, top loading balance; 9, cyclone; 10, sampling bottle; and 11, bag filter.

Table 1. Physical Properties of the Solid Particles

	Alumina		C/B[a]		
	F-150	F-220	HI-900L	PVC	glass beads
true density	3980 kg/m^3	3980 kg/m^3	2200 kg/m^3	1400 kg/m^3	2500 kg/m^3
bulk density	1834 kg/m^3	1592 kg/m^3	220 kg/m^3	582 kg/m^3	1476 kg/m^3
mean diameter	89.59 μm	52.64 μm	0.015 μm	171.1 μm	1000 μm
Geldart's classification	A	A	C	A	D

[a] Primary particle size: 15 nm (from the catalog by Korea Carbon Black Co.).

Entrainment experiments were performed at different gas velocities, as a function of the ratio of alumina/carbon black content, the reactor type, and the static bed height. The entire bed was mounted on a balance and weighed with its contents. The loss of weight was due to entrainment of fine powders. Figure 2 shows typical curves of the weight loss in the conical fluidized beds without a tube. The entrainment rate of fine powders was determined by measuring the initial weight loss

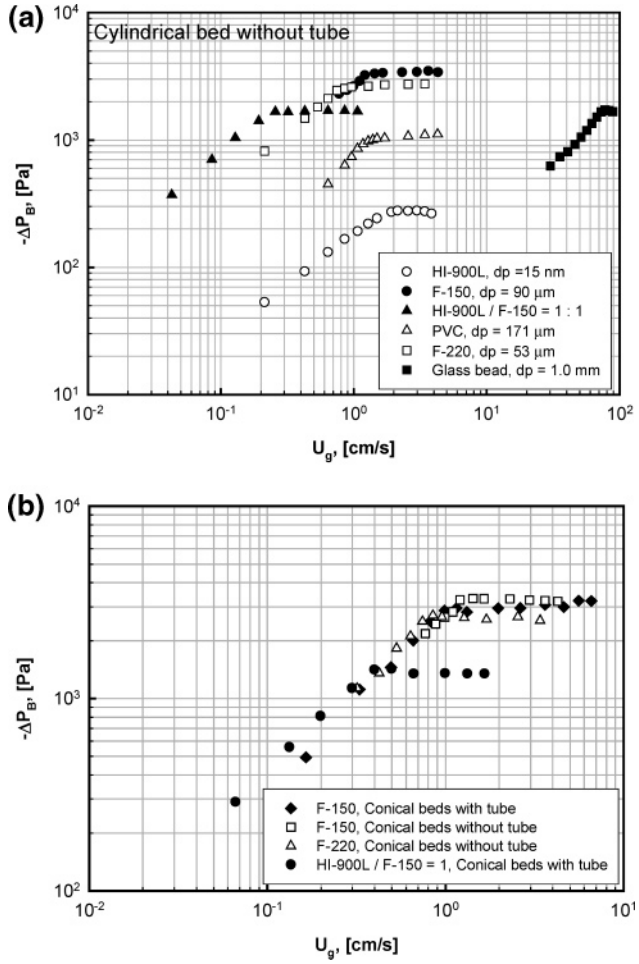

Figure 2. Variation of the pressure drop in the bed as a function of gas velocity in (a) cylindrical fluidized beds and (b) conical fluidized beds.

from the bed. The entrainment rate (W_i) is calculated from the following equation:

$$W_i = \frac{m}{\Delta t} = AK_i \tag{1}$$

where the entrainment rate constant (K_i) is defined as

$$K_i = \frac{m}{(\Delta t)A} = \frac{W_i}{A} \tag{2}$$

in which m is the mass of entrained fine powder, and A is the cross-sectional area of the reactor.

3. Results and Discussion

To determine the minimum fluidizing velocity of each particle, pressure drops ($-\Delta P_B$) in the bed with a static bed height of 0.2 m, relative to variation in the gas velocity in conical and cylindrical fluidized beds, were measured, as shown in Figure 3a and b. As can be seen, pressure drops in these beds increased as the gas velocity increased up to the minimum fluidizing condition and then stabilized. The slope of $-\Delta P_B$ for beds with different gas velocities in fixed beds is ~1.0, because the Ergun equation's prediction of the particle Reynolds number under minimum fluidization ($Re_{p,mf}$) conditions is proportionate to the gas velocity when the particle sizes are small and the particle density is low.[13] In Figure 3a, the U_{mf} value of F-150 is greater than that of F-220, because of the large particle diameter for the same alumina particles. Among all the particles, the U_{mf} value of glass beads ($d_p = 1.0$ mm) is the greatest. The minimum fluidization velocity of the mixture (HI-900L and F-150) is less than both that of the alumina of F-150 and that of the carbon black of Hi-900L, because the fine powders of Hi-900L are packed in the pores of the alumina (F-150) particles. Although the primary size of Hi-900L is 15 nm, these particles are agglomerated in the beds. The experimental U_{mf} value of HI-900L is 1.7 m/s. This value is high, in comparison with the estimated value of 1.56×10^{-10} m/s that is determined using the Wen and Yu equation, because the particles of HI-900L are agglomerated with each other. The measured minimum fluidization velocities of each particle are shown in Table 2.

The calculating entrainment rate (W_i), based on the output of fine particles at a given unit of time, at the gas velocity in the cylindrical fluidized beds with a tube is shown in Figure 4. The material in the beds is the mixture of alumina (F-150) and carbon black, where alumina is the medium particle and carbon black is the fine particle. As seen in Table 1, a single alumina particle is ~1000 times greater than the size of a carbon black particle. In the entrainment experiment, at a specific gas velocity, a portion of the carbon black is not separated as it attaches, but some particles are not attached to the alumina particle, and, thus, those are entrained outward from the reactor. Baron et al.[12] also mentioned that it is difficult to elutriate fine particles, because they aggregate via the cohesive force between themselves. As can be observed in Figure 4, the entrainment rate of carbon black particles increases as the gas velocity increases, because a high gas velocity may crush the aggregated carbon black particles and also separates carbon black particles from alumina particles in the bed. Nakagawa et al.[14] previously have reported that the entrainment rate increases as the gas velocity increases and it decreases with the content of fine powders in a circulating PPFB. Also, Li et al.[15] explained that the entrainment rate of fine powders decreases as the content of fine powder is increased, because interparticle forces affect the entrainment rate more than the shear force of the flowing gas.

The entrainment rates of carbon black (HI-900L), as a function of the carbon content in the solid mixture in the conical fluidized bed with a tube, is shown in Figure 5. As can be seen, the effect of fine content on the entrainment rate in the conical fluidized beds is unclear. Although, in the cylindrical fluidized beds, the entrainment rate of carbon black increases as the gas velocity increases, it decreases as the content of carbon black in the solid mixture decreased, as observed previously by Nakagawa et al.[14] and Li et al.[15] Further work is needed to confirm the effect of fine content on the entrainment rate in the conical fluidized beds.

The entrainment rate constant of carbon powders from the conical and cylindrical fluidized beds, under the same operating conditions, is shown in Figure 6. The entrainment rate constant is calculated by eq 2, which considers the cross-sectional area of the bed. As can be observed, the entrainment rate constant from the cylindrical reactor is ~5−12 times greater than that from the conical fluidized bed at the given powder content and volumetric gas flow rate, because, in the conical reactor, the gas velocity decreases as gas rises upward through the reactor. Particles then reflux to the upper portion of the bed if the terminal velocity of the carbon black agglomerates is greater than the superficial gas velocity. However, in the case of a cylindrical reactor, most of the entrained particles do not reflux but are entrained, because the superficial gas velocity is constant from the distributor to the exit. In developing continuous hydrogen manufacturing processes through the direct decarbonization of hydrocarbon, entrainment of significant amounts

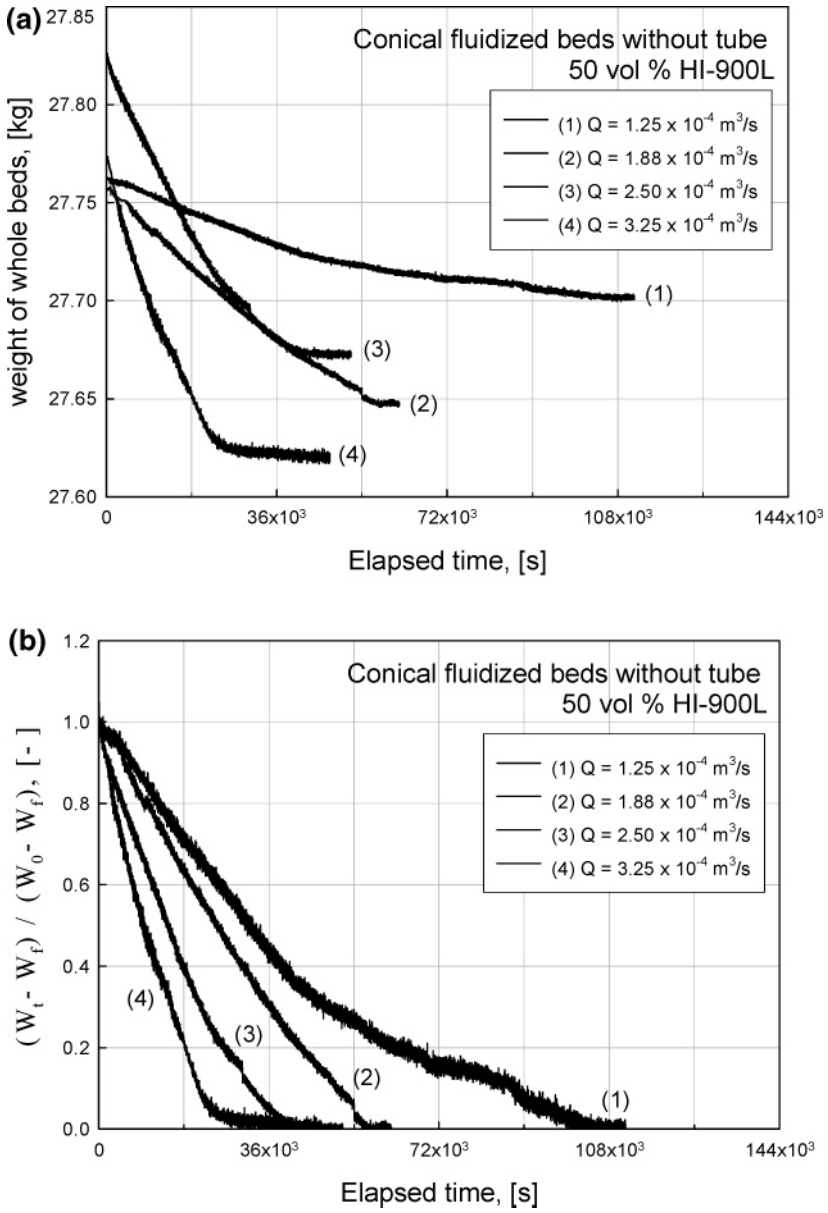

Figure 3. Variation of (a) the weight of whole beds and (b) the relative weight of the bed material, as a function of the elapsed time.

Table 2. Summary of U_{mf} for Various Particles

	Alumina				
	F-220	F-150	PVC	glass beads	HI-900L
mean diameter	52.94 μm	89.59 μm	171.1 μm	1000 μm	15 nm
true density	3980 kg/m^3	3980 kg/m^3	1400 kg/m^3	2500 kg/m^3	2100 kg/m^3
bulk density	1529 kg/m^3	1834 kg/m^3	582.1 kg/m^3	1476 kg/m^3	217.0 kg/m^3
$(Re_{mf})_{exp}$	0.030	0.086	0.146	49.0	1.7×10^{-5}
$(U_{mf})_{exp}$	0.855 cm/s	1.436 cm/s	1.282 cm/s	73.5 cm/s	1.7 cm/s

of the carbon black created is indispensable, because the accumulation of the carbon black created in the reactor causes an increase of pressure inside the reactor and the reaction cannot proceed effectively. The reactor type is selected based on the required entrainment rate constant. In the beginning of the reactor development, a conical-type reactor was selected, because of its segregation-preventive property. However, it was substituted by a cylindrical reactor, because the entrainment rate constant was significantly lower than the required one. Therefore, we can claim that a cylindrical fluidized bed is better than a conical fluidized bed for the continuous process of hydrogen manufacturing.

The entrainment rate constants are shown in Figure 7, as a function of static bed height (0.2−0.4 m). The mixing ratio of the media and fine particles in the fluidized beds is 50:50 by volume. Although the entrainment rate constant with 0.3 m is higher than that with 0.2 m at all of the gas velocities, there is not much difference in entrainment at each height at different gas velocities. The entrainment rate seems to be constant by changing the static bed height. Many correlations of the elutriation rate constant have been proposed by various investigators. Table 3 shows the most representative correlations. These predicted values differ greatly from each other. A comparison between experiment and existing correlations is

Table 3. Previous Correlations for Elutriation Rate Constant, *K*

investigators	Experimental Conditions: d_f [m]	d_{pc} [μm]	d_{pi} [μm]	U_g [m/s]	Geldart group	correlation for K_i
Yogi and Aochi[16]	0.07−1.0	100−1600	80−300	0.3−1.0	A/B	$\frac{K_i g d_{pi}^{\ 2}}{\mu(U_g - U_t)} = 0.0015 Re_t^{0.6} + 0.01 Re_t^{1.2}$
Zenz and Weil[17]	0.05 × 0.61		20−150	0.3−0.72	A	$\frac{K_i}{\rho_g U_g} = 1.26 \times 10^7 \left(\frac{U_g^{\ 2}}{g d_{pi} \rho_p^{\ 2}}\right)^{1.87}$ $\left(\text{for } \frac{U_g^{\ 2}}{g d_{pi} \rho_p^{\ 2}} \le 3.63 \times 10^{-2}\right)$ $\frac{K_i}{\rho_g U_g} = 4.31 \times 10^4 \left(\frac{U_g^{\ 2}}{g d_{pi} \rho_p^{\ 2}}\right)^{1.18}$ $\left(\text{for } \frac{U_g^{\ 2}}{g d_{pi} \rho_p^{\ 2}} \ge 3.63 \times 10^{-2}\right)$
Tanaka et al.[18]	0.031−0.067	718−1930	106−505	0.9−2.8	A/B	$\frac{K_i}{\rho_g (U_g - U_t)} = 0.046 \left[\frac{U_g - U_t}{(g d_{pi})^{0.5}}\right] Re^{0.3} \left(\frac{\rho_p - \rho_g}{\rho_g}\right)^{0.15}$
Geldart et al.[19]	0.076−0.3	350−1500	60−300	0.6−3.0	A/B	$\frac{K_i}{\rho_g U_g} = 23.7 \exp\left[-5.4 \left(\frac{U_t}{U_g}\right)\right]$
Colakyan and Levenspiel[10]	0.92 × 0.92, 0.3 × 0.3	300−1000	36−542	0.90−3.66	A/B	$K_i = 0.011 \rho_p \left(1 - \frac{U_t}{U_g}\right)^2$
Baeyens et al.[21]	0.08	30−77.8	10.1−13.9	0.2−0.7	A/C	$K_i = 5.4 \times 10^{-5} \rho_p \left(\frac{U_g}{0.2}\right)^{3.4} \left(1 - \frac{U_t}{U_g}\right)^2$ $(\text{for } d_{pi} < d_{crit})$
Ma and Kato[22]	0.071	331	9.5−88	0.3−0.9	A/C	$\frac{K_i}{\rho_g (U_g - U_t)} = 5.38 \left[\frac{d_p (U_g - U_t) \rho_g}{\mu}\right]^{2.22} \left(\frac{0.45 \rho_p^{\ 0.269}}{\rho_p d_p g}\right)^{-0.15}$
Li and Kato[5]	0.1	69−650	12−91	0.3−0.7	A/C	$K_i = 6.64 \times 10^6 C_{ps} \left(\frac{\rho_g U_g g}{\rho_p}\right)^{2.64}$ $(\text{for } d_{pi} \le d_{crit})$ where $C_{ps} = 1$ $(\text{for } d_p \le 60\ \mu\text{m})$ $C_{ps} = \left(\frac{200 - d_p}{150}\right)^{\alpha} + \left(\frac{d_p - 60}{150}\right)^{\alpha} \left(\frac{d_{pi}}{d_{crit}}\right)^{1.4}$ $(\text{for } 60\ \mu\text{m} \le d_p \le 200\ \mu\text{m})$ Here, $\left(\frac{d_{pi}}{d_{crit}}\right)^{1.4}$ $(\text{for } d_p \le 200\ \mu\text{m})$ $\alpha = \left(\frac{d_{crit}}{d_{pi}}\right)^{0.3}$ and $d_{crit} = \frac{1.01 \times 10^5}{\rho_p g^{0.731}}$

shown in Figure 7. As can be seen in Figure 7, the correlation of the elutriation rate constant using Geldart group A or B particles is not matched between experiments and predicted values. However, the correlation of the elutriation rate constant by Li and Kato[5] is well-matched, because they used the Geldart group A or group C particles as fine powders. Further work is needed to confirm theoretically the entrainment rate constant for the Geldart group C powders.

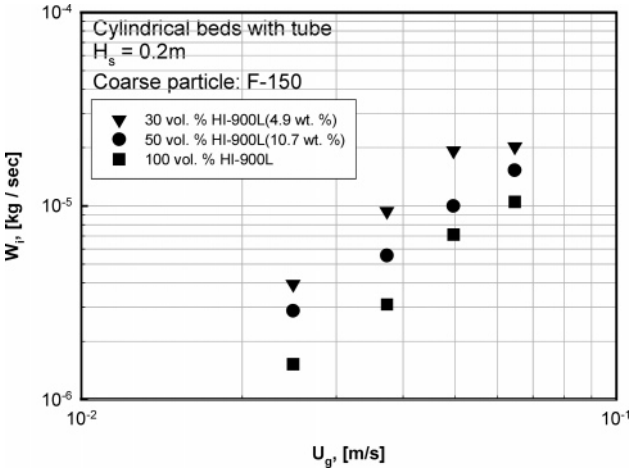

Figure 4. Variation of the entrainment rate in the mixture of particles, as a function of gas velocity in cylindrical beds.

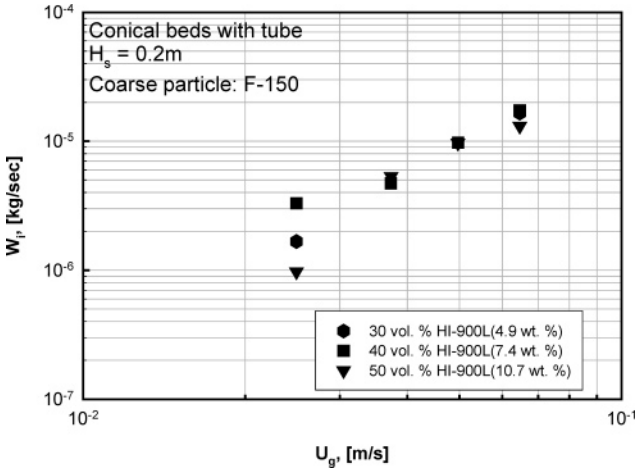

Figure 5. Variation of the entrainment rate in the mixture of particles (F-150 and HI-900L), as a function of gas velocity in conical beds.

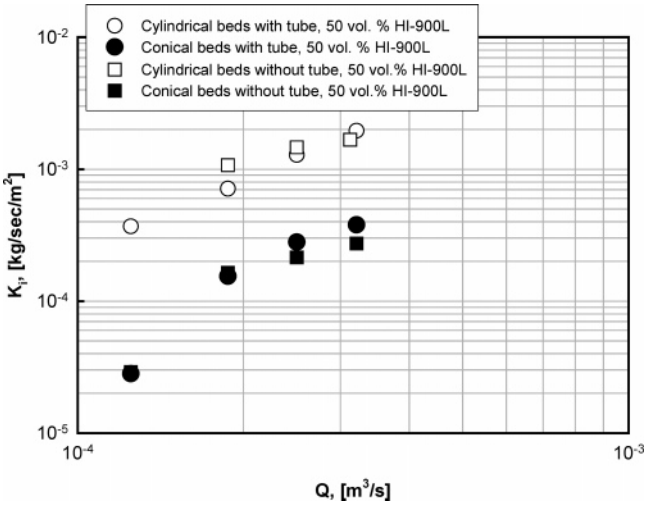

Figure 6. Variation of the entrainment rate constant with the volumetric gas flow rate in the conical and cylindrical fluidized beds with or without a tube.

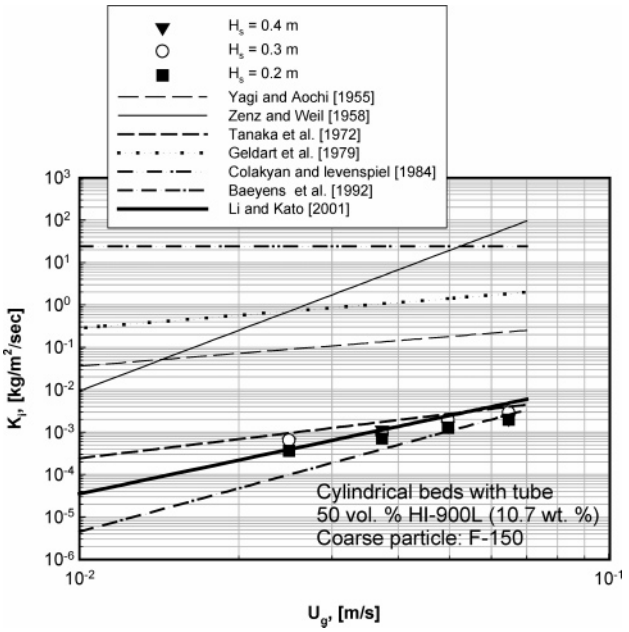

Figure 7. Variation of the entrainment rate constant in cylindrical beds, as a function of the height of the static bed.

4. Conclusions

The entrainment rate of carbon black powder increases as the gas velocity increases, but it decreases as the content of fine powder in the mixture in the cylindrical fluidized beds increases. However, the effect of fines content on the entrainment rate in the conical fluidized beds is unclear. Further work is needed to confirm the effect of fines content on the entrainment rate in the conical fluidized beds. The entrainment rate constant of carbon black powder from the cylindrical fluidized-bed reactor is 5−12 times greater than that from the conical inert-medium fluidized-bed reactor. The cylindrical inert-medium fluidized-bed reactor is observed to be better than the conical fluidized-bed reactor for a continuous hydrogen manufacturing process. The entrainment rate seems to be constant by changing the static bed height. Further work is needed to confirm the entrainment rate constant for the Geldart group C powders theoretically.

This study was supported by "National RD&D Organization for Hydrogen & Fuel Cell" and "Ministry of Commerce, Industry and Energy".

Nomenclature

A = freeboard cross-sectional area in the beds [m^2]
C_{ps} = particle size coefficient
d_{crit} = critical size at which interparticle forces dominate [μm]
d_p = mean diameter of bed particle [μm]
d_{pc} = diameter of coarse particle [μm]
d_{pi} = diameter of fine powder [μm]
d_t = column diameter [m]
g = gravitational acceleration [m/s^2]
H_s = static bed height [m]
K_i = entrainment rate constant [kg/m^2/s]
m = mass of entrained fine powder [kg]
Q = volumetric gas flow rate [m^3/s]
Re_{mf} = Reynolds number under minimum fluidizing conditions
Re_t = Reynolds number at terminal velocity for particle diameter d_{pi}
U_g = superficial gas velocity [m/s]
U_{mf} = minimum fluidization velocity [m/s]
U_t = terminal velocity [m/s]
W_0 = weight of the initial bed material [kg]
W_f = weight of the final bed material [kg]
W_i = entrainment rate [kg/s]
W_t = weight of the instantaneous bed material [kg]

Greek Symbols

α = particle ratio of d_{crit} to d_{pi}
$-\Delta P_B$ = pressure drop of the beds [Pa]
Δt = time interval [s]
μ = gas viscosity [Pa s]
ρ_g = gas density [kg/m^3]
ρ_p = particle density [kg/m^3]

Literature Cited

(1) Wen, C. Y.; Hashinger, R. F. Entrainment of Solid Particles from a Dense-phase Fluidized Bed. *AIChE J.* **1960**, *6*, 220.

(2) Wen, C. Y.; Chen, L. H. Fluidized Bed Freeboard Phenomena: Entrainment and Elutriation. *AIChE J.* **1982**, *28*, 117.

(3) Li, J. L.; Yamashida, A.; Kato, K. Entrainment of Very Fine Particles from Fluidized Beds-Effect of Mean Diameter of Bed Particles. *J. Chem. Eng. Jpn.* **2000**, *33*, 730.

(4) Li, J. L.; Kato, K. Estimation of the Critical Particle Size of Entrainment of Very Small Particles from Fluidized Bed. *J. Chem. Eng. Jpn.* **2001,** *34* (7), 892.

(5) Li, J. L.; Kato, K. A. Correlation of the Entrainment Rate Constant for Adhesion Particles (Group C Particles). *Powder Technol.* **2001**, *118*, 209.

(6) Kato, K.; Takarada, T.; Koshinuma, A.; Kanazawa, I.; Sugihara, T. Decarbonization of Silicon Carbide−Carbon Fine Particles Mixture in a Fluidized Bed. In *Fluidization VI*; Grace, J. R., Shemilt, L., Bergougnou, W. M. A., Eds.; Engineering Foundation: New York, 1989.

(7) Nakagawa, N.; Ohsawa, K.; Takarada, T.; Kato, K. Continuous Drying of Fine Particle-Water Slurry in a Powder-Particle Fluidized Bed. *J. Chem. Eng. Jpn.* **1992**, *25*, 495.

(8) Takarada, T.; Tonishi, T.; Takezawa, H.; Kato, K. Pyrolysis of Yallourn Coal in a Powder−Particle Fluidized Bed. *Fuel* **1992**, *71*, 1087.

(9) Wang, C.; Machida, H.; Nakagawa, N.; Takarada, T.; Kato, K. Catalytic Pyrolysis of Plant-Biomass in a Powder-Particle Fluidized-Bed. *Kagaku Kogaku Ronbunshu* **1995**, *21*, 531.

(10) Gao, S.; Nakagawa, N.; Kato, K.; Inomato, M.; Tsuchiya, F. Simultaneous SO_2/NO_x Removal by a Powder-Particle Fluidized Bed. *Catal. Today* **1996**, *29*, 165.

(11) Geldart, D.; Wong, A. C. Y. Entrainment of Particle from Fluidized Beds of Fine Powder. *AIChE Symp. Ser.* **1987**, *83*, 1.

(12) Baron, T.; Briens, C. L.; Hazlett, J. D.; Bergougnou, M. A.; Galtier, P. Size distribution of the particles entrained from fluidized bed: gas humidity effects. *Can. J. Chem. Eng.* **1992**, *70*, 631.

(13) Ergun, S. Fluid Flow through Packed Columns. *Chem. Eng. Progr.* **1952**, *48*, 89.

(14) Nakagawa, N.; Mahmoud, E. A.; Nakazato, N.; Kato, K. Evaluation of the Turnover Times of the Bed Particles and the Fine Powders in a Circulating Powder-Particle Fluidized Bed. *Powder Technol.* **2005**, *153*, 81.

(15) Li, J.; Nakazato, T.; Kato, K. Effect of Cohesive Powders on the Entrainment of Particles from a Fluid Bed. *Chem. Eng. Sci.* **2004**, *59*, 2777.

(16) Yagi, S.; Aochi, T. Elutriation of Particles from a Batch Fluidized Bed. In *Proceedings of the Spring Meeting of the Society of Chemical Engineers, Japan*, 1955; p 89.

(17) Zenz, F. A.; Weil, N. A. A Theoretical-Empirical Approach to the Mechanism of Particle Entrainment from Fluidized Beds. *AIChE J.* **1958**, *4*, 472.

(18) Tanaka, I.; Shinohara, H.; Hirosue, H.; Tanaka, Y. Elutriation of Fines from Fluidized Bed. *J. Chem. Eng. Jpn.* **1972**, *5*, 51.

(19) Geldart, D.; Cullian, J.; Georghiades, S.; Gilvray, D.; Pope, D. J. The Effect of Fines on Entrainment of Gas Fluidized Beds. *Trans. Inst. Chem. Eng.* **1979**, *57*, 269.

(20) Colakyan, M.; Levenspiel, O. Elutriation from Fluidized Bed. *Powder Technol.* **1984**, *38*, 223.

(21) Baeyens, J.; Geldart, D.; Wu, S. Y. Elutriation of Fines from Gas Fluidized Beds of Geldart A-type Powders—Effect of Adding Superfines. *Powder Technol.* **1992**, *71*, 71.

(22) Ma, X. X.; Kato, K. Effect of Interparticle Adhesion Forces on Elutriation of Fine Powders from Fluidized Bed of Binary Particle-Mixture. *Powder Technol.* **1998**, *95*, 93.

Received for review August 19, 2006
Revised manuscript received December 8, 2006
Accepted December 19, 2006

IE061098E